# A Multi-domain Magneto Tunnel Junction for Racetrack Nanowire Strips

Prayash Dutta, Albert Lee, *Student Member, IEEE*, Kang L. Wang, *Fellow, IEEE*, Alex K. Jones, *Senior Member, IEEE*, and Sanjukta Bhanja, *Senior Member, IEEE* 

Abstract—Domain-wall memory (DWM) has SRAM class access performance, low energy, high endurance, high density, and CMOS compatibility. Recently, shift reliability and processing-using-memory (PuM) proposals developed a need to count the number of parallel or anti-parallel domains in a portion of the DWM nanowire. In this paper we propose a multi-domain magneto-tunnel junction (MTJ) that can detect different resistance levels as a function of a the number of parallel or anti-parallel domains. Using detailed micromagnetic simulation with LLG, we demonstrate the multi-domain MTJ, study the benefit of its macro-size on resilience to process variation and present a macro-model for scaling the size of the multi-domain MTJ. Our results indicate scalability to seven-domains while maintaining a  $16.3\,\mathrm{mV}$  sense margin.

Index Terms—Spintronics, Domain wall memory

#### I. INTRODUCTION

**D** OMAIN-wall memory (DWM), or "Racetrack" memory [1], is among the most promising new memory technologies. As a spintronic memory it inherits the SRAM class access performance and low energy of STT-MRAM with a dramatically higher density (as small as  $2F^2$ , where F is the technology feature size). Moreover, DWM avoids endurance challenges by providing  $\geq 10^{16}$  write cycles [1] compared to endurance limited phase-change and resistive memories at  $10^8-10^9$  and  $10^{11}-10^{12}$  write cycles, respectively [1].

DWMs are ferromagnetic nanowires. DWM nanowires extend the free-layer to store multiple, *e.g.*, 32-512, magnetically polarized domains that correspond to bits, separated by fabricated triangular notches. Between adjacent domains storing complimentary bits, a mobile *domain wall* (DW) that pins to these notches balances the exchange and anisotropic energies. Spin-polarized current can shift the magnetic domains with controlled DW motion. DWM's improved density comes at the cost of this data shifting, which is necessary to align data with access points, which are magnetic tunnel junctions (MTJ). There has been significant effort on power reduction and speed improvement [1], [2] to optimize DWM shifting overhead and others to address shift reliability [3], [4].

Transverse read [5] has recently been proposed to count the number of parallel or anti-parallel (i.e., count of '1's)

Manuscript received May 24, 2022; revised September 21, 2022; revised January 6, 2023.

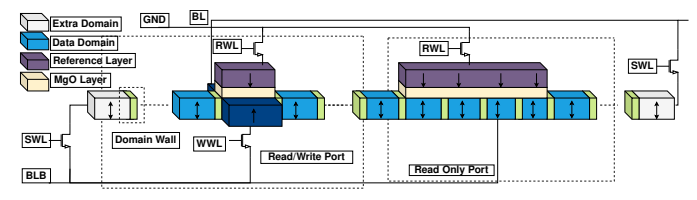


Fig. 1: Anatomy of a DWM nanowire for multi-domain read.

between two access ports of the nanowire with applications to shifting fault tolerance [4] and processing-in-memory [6]. It applies a much smaller than a shifting current,  $R_T << R_S$  across BLB and GND by opening WWL in Fig. 1 to detect the tunneling magnetoresistance (TMR) of multiple domains against the fixed layer of an MTJ, e.g., the read-only access port shown in dark blue. However, proximity of the domain to the tunneling effect can create variation in the resistance for different permutations of data and limit the scalability of how many domains can be sensed. Furthermore, this structure is likely sensitive to process variation. Thus, we propose a multi-domain magneto tunnel junction device that can count the number of 1's in a segment of the nanowire while having the potential for improved scalability and better resiliency to process variation.

## II. MULTI-DOMAIN MAGNETO TUNNEL JUNCTION

Our proposed multi-domain MTJ is shown in Fig. 2. The multi-domain MTJ is similar to the read-only access port from Fig. 1 except visualized with the fixed layer and MgO below the free layer and covering multiple domains. The system behaves like k parallel resistors where k is the number of domains covered by the multi-domain MTJ. Each domain's region forms a high or low resistance state depending on parallel (-Z) or anti-parallel (+Z) magnetic polarization. Thus, the multi-domain MTJ resistance is determined by the number of parallel (or anti-parallel) domains, representing how many, but not which domains store '1's.

Prior work has used a spintronic nanowire with a flexible DW to store an analog weight for neural network processing [7]. This requires fine control over the DW motion and high precision sense-amplifiers to detect different analog values. While there are some smaller effects which do perturb the resistance levels based on the actual pattern of '1's in the device, our multi-domain MTJ uses notches to ensure domain stability while shifting and functions as digital device. Z-direction current applied evenly across the multi-domain MTJ can induce flow in the +/-X direction to seek lower resistance paths inducing some Anisotropic Magenetoresistance (AMR). Additionally, DW regions have different resistance properties.

P. Dutta and S. Bhanja are with University of South Florida, Tampa, FL 33620, USA e-mail: {prayash,bhanja}@usf.edu.

A. Lee and K. L. Wang are with the ECE Department, University of California at Los Angeles, Los Angeles, CA 90095, USA e-mail: {alee0618,klwang}@ucla.edu.

A. K. Jones is with the ECE Department, University of Pittsburgh, Pittsburgh, PA 15261, USA email: akjones@pitt.edu

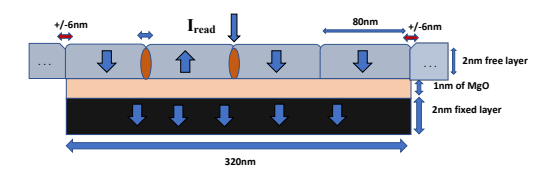


Fig. 2: The experimental setup. The brown ellipses are the domain walls between two oppositely magnetized domains.

TABLE I: Multi-domain MTJ Properties and Dimensions

Property		Values		
Fixed and Free Layer Material		CoFeB		
Fixed and Free Layer Size		$320\mathrm{nm}\times40\mathrm{nm}\times2\mathrm{nm}$		
Domain Size		$80\mathrm{nm}\times40\mathrm{nm}\times2\mathrm{nm}$		
Notch dimensions (triangular)		$12\mathrm{nm}\times10\mathrm{nm}\times2\mathrm{nm}$		
MgO Layer Size		$320\mathrm{nm}\times40\mathrm{nm}\times1\mathrm{nm}$		
CoFeB Parameters		$K_u$	$99999\mathrm{erg/cc}$	
AMR Ratio	0.014	Ms	1200 emu/cc	
Resistivity	$15 \mu\Omega$ cm	Exchange Stiffness	$2.2\mu\mathrm{erg/cm}$	
MgO TMR Ratio	0.8	$J_C$	$3.21 \times 10^{10} \text{A/m}^2$	

Thus, domains containing "1010" will have slightly different resistance than than "1100" due to different numbers of DWs. Because the multi-domain MTJ is much larger than F, we expect variation to only impact the device at the extremities, creating a small amount of under- or over-hang of boundary domain notches, while the internal domains are covered in their entirety. Thus, the impact is less significant than when aligning a single MTJ to a single DWM domain or detecting the resistance with a freely moving DW.

### III. EXPERIMENTAL SETUP AND RESULTS

We simulated the multi-layer structure from Fig. 2 using the LLG micromagentic simulator [8] using CoFeB and MgO at temperature  $300\,\mathrm{K}$  with the parameters shown in Table I.  $K_u$  is the uniaxial anisotropy and Ms is the saturation magnetization. Domains were of  $80\,\mathrm{nm}$  long,  $40\,\mathrm{nm}$  wide, and  $2\,\mathrm{nm}$  thick. 4 domains were included in the MTJ with a 1 nm thick MgO layer and  $2\,\mathrm{nm}$  thick CoFeB fixed layer. Triangular notches of size  $12\,\mathrm{nm} \times 10\,\mathrm{nm} \times 2\,\mathrm{nm}$  create pinning sites for DWs. All results are an average of 10 simulations and are tightly convergent. The maximum standard deviation for  $300\,\mathrm{K}$  is  $0.14\,\Omega$  for "0101" combination.

The fixed layer is magnetized in the -Z direction. Each free layer domains can be magnetized in either +/-Z. The MgO layer is a non-magnetic tunneling barrier. We assign +Z (antiparallel, high resistance) as '1' and -Z (parallel, low resistance) as '0'. Our read current  $(I_{read})$  has a read current density  $J_c = 3.21 \times 10^{10} A/m^2$  and remains an order of magnitude lower than the switching current density to minimize the potential of read disturbance [9]. For our 3 ns read access time, the read energy is  $0.5 \, \mathrm{pJ}$ . For more than four domains,  $I_{read}$  can increase to keep  $J_C$  invariant. We attempted to match experimental parameters with prior transverse read work [5].

The resistance is measured from the top of the free layer to the bottom of the fixed layer in the simulator which originates TMR effects from the MTJ and AMR effects from DWs. The impact of domain contents on voltage is shown graphically in blue based on micromagnetic simulation in Fig. 3. We see good similarity of the voltages for all combinations with the same '1's count and the margin between clusters grows as the number of '1's increases. Variability in the cluster is primarily due to the number of DWs. The minimum margin is  $33.5\,\mathrm{mV}$ 

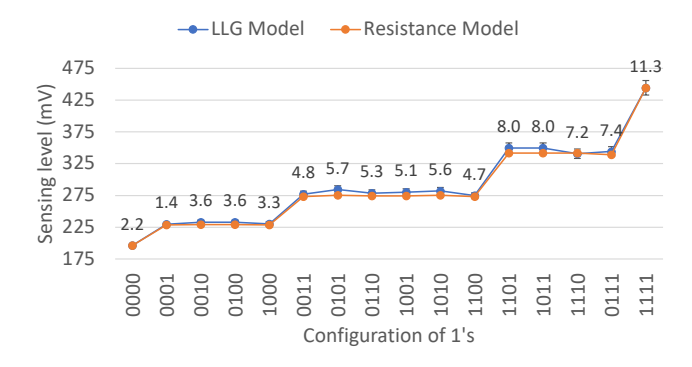


Fig. 3: Sense margin for all permutations of four domains in the free layer. Error bars and labels report  $6\sigma$  error deviation. between "0000" and "0001," which well exceeds the minimum margins of practical sense amplifiers [10]. The margin grows between groups with more '1's.

Thermal sensitivity: We conducted a sensitivity study of the 16 combinations for three different temperatures  $250\,\mathrm{K}$ ,  $300\,\mathrm{K}$ , and  $350\,\mathrm{K}$ . There was no magnetic change nor domain-wall movement when applying thermal fluctuations during simulation [10]. The average standard deviation for all combinations is  $0.07\Omega$  where the maximum standard deviation is  $0.31\Omega$  for "1101" (at  $350\,\mathrm{K}$ ), that reduces to  $0.12\,\Omega$  for 1000 runs. The minimum resistance gap for this multi-domain read sense amplifier is  $77.5\,\Omega$ , which requires a worst-case sense margin of  $31.8\,\mathrm{mV}$  to be accurately sensed, which is only nominally  $(1.7\,\mathrm{mV})$  different than the  $300\,\mathrm{K}$  only results.

**Process variation:** We simulated with a  $2 \, \mathrm{nm}$  and  $6 \, \mathrm{nm}$  misalignment between the notch in the extended free layer and the MgO and CoFeB fixed layer (red arrows in Fig. 2), where we treated  $5.5 \, \mathrm{nm}$  as the  $6\sigma$  in a standard distribution of variation [11]. The MgO and CoFeB fixed layer would be fabricated with trenches and etching followed by chemical vapor deposition of doped CoFeB and MgO. The alignment concern would come from the location of the notch with the trench wall. The sense margin deviation for  $6 \, \mathrm{nm}$  is shown with error bars to the blue series in Fig. 3. As the error bars are small we also report this deviation in mV as labels. From our read current density, the lowest voltage level that has to be recognized for this resistance gap is still a healthy  $28.4 \, \mathrm{mV}$ .

Notch variations: Another form of process variation is changes to the notch dimension. Using a variation up to 8.4%. the minimum resistance gap for the worst-case scenario is  $72.53\,\Omega$ . This minimally impacts the required sense margin from the baseline to  $29.8\,\mathrm{mV}$ . The analysis of thermal effects and process variation (over-/under-hang of the free layers and notch dimension variation) show minimal impact on the sensing margin and provide confidence that our multi-domain read method is resilient and robust to these concerns.

### IV. ANALYTICAL MODEL AND SCALING

Detailed magnetic modeling with LLG becomes impractical as number of domains scales. Like prior approaches for analog DW movement in a nanowire [12] and spintronic logic proposals [13], we have constructed a characterized analytical model of the multi-domain MTJ which we describe in Fig. 4. This entire model is a parallel arrangement of some mini-resistive structures. The 4-domain example shown in the figure shows

$$J_C D A_d \left\{ \left( \frac{D-2}{R_{80}^-} + \frac{1}{R_{74}^-} + \frac{1}{R_{68}^+} + \frac{1}{R_{68}^{DW}} + \frac{1}{R_{68}^{hDW}} \right)^{-1} - \left( \frac{D-2}{R_{80}^-} + \frac{2}{R_{74}^-} + \frac{2}{R_{-Z}^{hDW}} \right)^{-1} \right\}$$
(1)

a "0001" but both bordering values are different. Thus, the leftmost domain has a low resistance configuration, denoted  $R^-$  for  $74\,\mathrm{nm}$  and half a DW. The next domain has  $R^-$  for  $80\,\mathrm{nm}$ , followed by  $R^-$  for  $74\,\mathrm{nm}$ , a full DW, and  $R^+$  for  $68\,\mathrm{nm}$ , with another half DW. From characterization these can be converted to particular resistance values shown in Table II. We can scale to a five-domain MTJ by adding the shaded fixed and barrier layers in Fig. 4 modeling "00010." The expression replaces the rightmost half DW with a full DW and another  $R^-$  for  $74\,\mathrm{nm}$ . These divisions are segmented by red dotted lines with black lines indicating the borders of the 4-domain and 5-domain examples. "00010" can be calculated through the parallel equivalent resistance to be  $431.5\,\Omega$ .

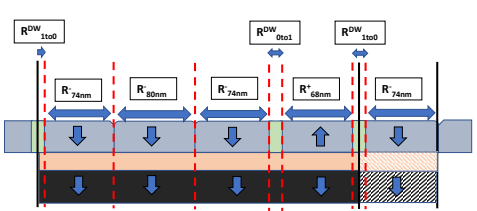


Fig. 4: Resistance modeling of domains in the free layer

TABLE II: Simulation mini structures and resistance

Direction: Size	Notation	Resistance (Ω)	
- <b>Z</b> : 80 nm, 74 nm, 68 nm	$R_{80}^-, R_{74}^-, R_{68}^-$	1911, 2048, 2228	
<b>+Z</b> : 80 nm, 74 nm, 68 nm	$R_{80}^+, R_{74}^+, R_{68}^+$	4324, 4730, 5143	
<b>DW</b> -Z to +Z, +Z to -Z: 12 nm	$R_{0\rightarrow1}^{DW}, R_{1\rightarrow0}^{DW}$	20053, 20063	
<b>Half DW</b> -Z to $Z_{\emptyset}$ , +Z to $Z_{\emptyset}$ : 6 nm	$R_{-Z}^{hDW}, R_{+Z}^{hDW}$	35061, 46196	

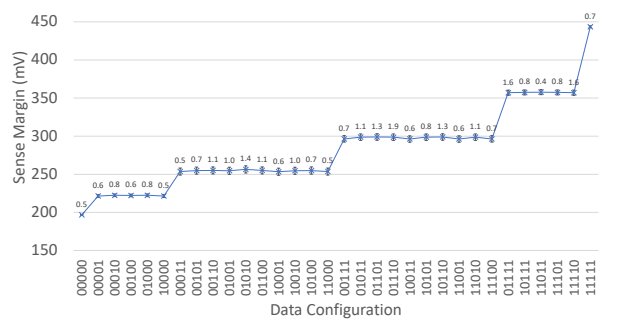


Fig. 5: 5-domain MTJ. Labels report variation due to neighboring domains.

We demonstrate accuracy of matching this model to the micromagnetic simulation data for a four domain MTJ in the orange series of Fig. 3, which has an average and maximum error of 1.4% and 3.2%, respectively. We also show data from the five-bit domain model with resistances presented in Table III and sensing margins presented in Fig. 5. We checked data for different numbers of '1's through micromagnetic simulation and determined an average error of < 1%. This data demonstrates six different distinguishable levels when applying the same  $J_C$  projects a minimum sense margin is  $23.7\,\mathrm{mV}$ , which remains detectable by standard sense amplifiers [10]. We can represent the minimum sense margin as described in Eq. 1 where D is the number of domains in the multi-domain

 Combination
 Resistance
 Combination
 Resistance

 All 0's ↓
 Three 1's ↓

 00000
 382.10
 00111, 11100
 576.22

TABLE III: Projected Five-domain Resistances

00000	302.10	00111, 11100	370.22
One 1's ↓		01011, 11010	580.11
00001, 10000	431.07	01101, 10110	581.07
00010, 00100, 01000	431.50	01110, 10011, 11001	577.94
Two 1's ↓		10101	583.27
00011, 11000	493.19	Four 1's ↓	
00101, 10100	496.03	01111, 11110	692.87
00110, 01100, 10001	494.45	10111, 11011, 11110	697.39
01001, 10010	495.01	Four 1's ↓	
01010	496.6	11111	864 88

MTJ,  $A_d$  is the area per domain, and values of R are found in Table II. For six and seven domains, the minimum margin scales to a still detectable  $19.3 \,\mathrm{mV}$  and  $16.3 \,\mathrm{mV}$ , respectively.

#### V. CONCLUSION

In this paper, we have proposed a process variation resilient novel technique to count the number of '1's in a DWM nanowire segment with an analytical model that allows to explore around more domain configurations.

#### REFERENCES

- [1] R. Bläsing, A. A. Khan, P. C. Filippou, C. Garg, F. Hameed, J. Castrillon, and S. S. P. Parkin, "Magnetic racetrack memory: From physics to the cusp of applications within a decade," *Proceedings of the IEEE*, vol. 108, no. 8, pp. 1303–1321, 2020.
- [2] R. Venkatesan, V. Kozhikkottu, C. Augustine, A. Raychowdhury, K. Roy, and A. Raghunathan, "Tapecache: a high density, energy efficient cache based on domain wall memory," in *Proc. of ISLPED*, pp. 185–190, 2012.
- [3] C. Zhang, G. Sun, X. Zhang, W. Zhang, W. Zhao, T. Wang, Y. Liang, Y. Liu, Y. Wang, and J. Shu, "Hi-fi playback: Tolerating position errors in shift operations of racetrack memory," in *Proc. of ISCA*, 2015.
- [4] S. Ollivier, S. Longofono, P. Dutta, J. Hu, S. Bhanja, and A. K. Jones, "Toward comprehensive shifting fault tolerance for domain-wall memories with piett," *IEEE Transactions on Computers*, pp. 1–14, 2022.
- [5] K. Roxy, S. Ollivier, A. Hoque, S. Longofono, A. K. Jones, and S. Bhanja, "A novel transverse read technique for domain-wall "race-track" memories," *IEEE TNANO*, vol. 19, pp. 648–652, 2020.
- [6] S. Ollivier, S. Longofono, P. Dutta, J. Hu, S. Bhanja, and A. K. Jones, "Coruscant: Fast efficient processing-in-racetrack memories," in *Proc. of MICRO*, Oct. 2022.
- [7] A. Sengupta, Y. Shim, and K. Roy, "Proposal for an all-spin artificial neural network: Emulating neural and synaptic functionalities through domain wall motion in ferromagnets," *IEEE TBioCAS*, vol. 10, no. 6, pp. 1152–1160, 2016.
- [8] M. Scheinfein, "Llg micromagnetics simulator," http://llgmicro.home. mindspring.com, vol. 18, p. 25, 1997.
- [9] D. H. Kang and M. Shin, "Critical switching current density of magnetic tunnel junction with shape perpendicular magnetic anisotropy through the combination of spin-transfer and spin-orbit torques," *Scientific re*ports, vol. 11, no. 1, pp. 1–8, 2021.
- [10] S. Salehi, D. Fan, and R. F. Demara, "Survey of stt-mram cell design strategies: Taxonomy and sense amplifier tradeoffs for resiliency," ACM JETC, vol. 13, no. 3, pp. 1–16, 2017.
- [11] M. Komalan, S. Sakhare, T. H. Bao, S. Rao, W. Kim, C. Tenllado, J. I. Gómez, G. S. Kar, A. Furnemont, and F. Catthoor, "Cross-layer design and analysis of a low power, high density stt-mram for embedded systems," in *Proc. of ISCAS*, pp. 1–4, IEEE, 2017.
- [12] C. Wang, Z. Wang, M. Wang, X. Zhang, Y. Zhang, and W. Zhao, "Compact model of dzyaloshinskii domain wall motion-based mtj for spin neural networks," *IEEE Transactions on Electron Devices*, vol. 67, no. 6, pp. 2621–2626, 2020.
- [13] X. Hu, A. Timm, W. H. Brigner, J. A. C. Incorvia, and J. S. Friedman, "Spice-only model for spin-transfer torque domain wall mtj logic," *IEEE Transactions on Electron Devices*, vol. 66, no. 6, pp. 2817–2821, 2019.